

---

This is an electronic reprint of the original article.  
This reprint may differ from the original in pagination and typographic detail.

Zhang, Yanpu; Batys, Piotr; O'Neal, Joshua T.; Li, Fei; Sammalkorpi, Maria; Lutkenhaus, Jodie L.

**Molecular Origin of the Glass Transition in Polyelectrolyte Assemblies**

*Published in:*  
ACS Central Science

*DOI:*  
[10.1021/acscentsci.8b00137](https://doi.org/10.1021/acscentsci.8b00137)

Published: 23/05/2018

*Document Version*  
Publisher's PDF, also known as Version of record

*Published under the following license:*  
Unspecified

*Please cite the original version:*  
Zhang, Y., Batys, P., O'Neal, J. T., Li, F., Sammalkorpi, M., & Lutkenhaus, J. L. (2018). Molecular Origin of the Glass Transition in Polyelectrolyte Assemblies. *ACS Central Science*, 4(5), 638-644.  
<https://doi.org/10.1021/acscentsci.8b00137>

---

This material is protected by copyright and other intellectual property rights, and duplication or sale of all or part of any of the repository collections is not permitted, except that material may be duplicated by you for your research use or educational purposes in electronic or print form. You must obtain permission for any other use. Electronic or print copies may not be offered, whether for sale or otherwise to anyone who is not an authorised user.

# Molecular Origin of the Glass Transition in Polyelectrolyte Assemblies

Yanpu Zhang,<sup>†</sup> Piotr Batys,<sup>§,⊥,||</sup> Joshua T. O’Neal,<sup>‡</sup> Fei Li,<sup>†</sup> Maria Sammalkorpi,<sup>\*,§</sup> and Jodie L. Lutkenhaus<sup>\*,†,‡,||</sup>

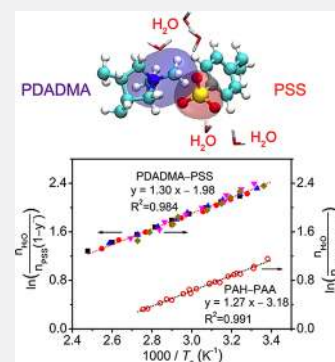
<sup>†</sup>Artie McFerrin Department of Chemical Engineering and <sup>‡</sup>Department of Materials Science and Engineering, Texas A&M University, College Station, Texas 77843, United States

<sup>§</sup>Department of Chemistry and Materials Science, <sup>⊥</sup>Department of Bioproducts and Biosystems, Aalto University, P.O. Box 16100, 00076 Aalto, Finland

<sup>||</sup>Jerzy Haber Institute of Catalysis and Surface Chemistry, Polish Academy of Sciences, Niezapominajek 8, PL-30239 Krakow, Poland

## Supporting Information

**ABSTRACT:** Water plays a central role in the assembly and the dynamics of charged systems such as proteins, enzymes, DNA, and surfactants. Yet it remains a challenge to resolve how water affects relaxation at a molecular level, particularly for assemblies of oppositely charged macromolecules. Here, the molecular origin of water’s influence on the glass transition is quantified for several charged macromolecular systems. It is revealed that the glass transition temperature ( $T_g$ ) is controlled by the number of water molecules surrounding an oppositely charged polyelectrolyte–polyelectrolyte intrinsic ion pair as  $1/T_g \sim \ln(n_{\text{H}_2\text{O}}/n_{\text{intrinsic ion pair}})$ . This relationship is found to be “general”, as it holds for two completely different types of charged systems (pH- and salt-sensitive) and for both polyelectrolyte complexes and polyelectrolyte multilayers, which are made by different paths. This suggests that water facilitates the relaxation of charged assemblies by reducing attractions between oppositely charged intrinsic ion pairs. This finding impacts current interpretations of relaxation dynamics in charged assemblies and points to water’s important contribution at the molecular level.



## INTRODUCTION

Charged assemblies bearing opposite or complementary charges span natural (proteins, enzymes, DNA)<sup>1–4</sup> to synthetic materials (surfactants, synthetic polyelectrolytes).<sup>5,6</sup> Assembly is facilitated by electrostatic attraction and entropic release of counterions, and most often occurs in aqueous media. These systems can range from solid-like to liquid-like, characteristic of the system relaxation dynamics. Similar to neutral macromolecules, charged assemblies can possess a  $T_g$ , which demarcates the glassy and rubbery states of the assembly. Notably decades ago, Michaels described synthetic polyelectrolyte complexes as brittle when dry but “leathery or rubberlike” when wet, which points to the strong effect of water on the mobility of a charged assembly.<sup>7</sup> Yet still there is not a clear view of how water facilitates the relaxation or, more specifically, controls the  $T_g$  of charged assemblies. To investigate this, we focus specifically upon synthetic polyelectrolyte complexes (PECs).<sup>8–10</sup>

The formation, structure, and properties of PECs are influenced by both the chemistry of the starting materials and the external conditions.<sup>11–19</sup> The resultant structure of the PEC, or for any charged assembly in general, is described in Figure 1. Polycations and polyanions assemble by forming intrinsic ion pairs, and the remaining unbound charged groups are compensated by small counterions to form extrinsic ion pairs. As this usually occurs in aqueous media, water molecules

surround various ion pairs in hydration layers. The extent of intrinsic ion pairing influences various physicochemical aspects such as conductivity, self-healing, and mechanical modulus.<sup>16,20,21</sup> Ion pairing also influences the  $T_g$ , which in turn defines their processability and applications as thermally responsive materials.<sup>22,23</sup>

Glass-transition-like thermal events have been identified in hydrated PECs and their counterparts, polyelectrolyte multilayers (PEMs). For PEMs, which are characterized more widely for their thermal behavior, the glass transition has manifested as a change in microcapsule or microtube size, heat capacity, mass, modulus, or impedance.<sup>24–27</sup> In all of these cases, water was present so as to achieve enough mobility to observe a  $T_g$ . The strong correlation between PEC/PEM physical properties and water has been noticed elsewhere.<sup>28–32</sup> These effects are generally attributed to water plasticization and a lowering of the  $T_g$  but the underlying mechanism needs further explanation.<sup>21,33</sup> This is because PECs possess mixed ion pairing character (intrinsic and extrinsic), and the location of water molecules and their states have not been fully quantified.<sup>34</sup>

Recently, we experimentally examined the thermal behavior of weak polyelectrolyte complexes consisting of poly(allylamine hydrochloride) and poly(acrylic acid) (PAH and PAA) as a

Received: March 2, 2018

Published: April 13, 2018

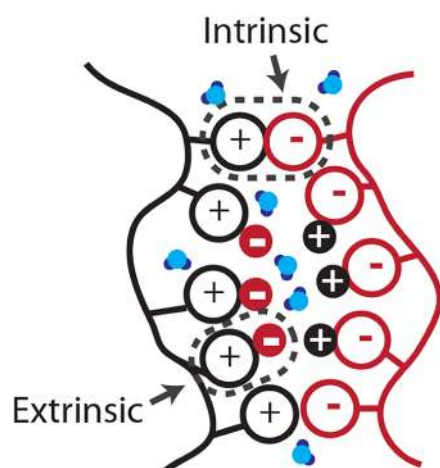


**Figure 1.** Schematic of a charged polyelectrolyte assembly. The charged polyelectrolyte assembly contains two different types of ion pairs: intrinsic and extrinsic. Intrinsic ion pairs are polycation–polyanion pairs, and extrinsic ion pairs are polyelectrolyte–counterion pairs.

function of pH (i.e., intrinsic ion pairing density) and water content. Glass transition-like behavior was observed, and the  $T_g$  was labeled as a generic thermal transition ( $T_{tr}$ ) since its mechanism was unclear. A correlation was speculated that connected  $T_g$  (or  $T_{tr}$ ) to the molar ratio of water to intrinsic ion pairs.<sup>35</sup> Our complementary simulation work for a different PEC system suggested that the observed thermally induced events were initiated by the changing dynamics of water molecules instead of a traditional glass transition event.<sup>36</sup> However, as this was only one study, it was not clear if this could be applied to other charged assemblies and even those made by different means.

Here, the  $T_g$  of synthetic PECs consisting of strong polyelectrolytes is correlated to the ratio of water molecules to intrinsic ion pairs. Strong polyelectrolytes are not sensitive to pH; rather, their intrinsic ion pairing is controlled by salt concentration. This is important as the prior correlation was only sensitive to pH, and here connections to salt concentration are made. Synthetic PECs consisting of poly(diallyldimethylammonium) and poly(styrenesulfonate) (PDADMA and PSS) are investigated using neutron activation analysis (NAA), modulated differential scanning calorimetry (DSC), and molecular dynamics (MD) simulation (see Supporting Information, Figures S1 and S2, Tables S1–S3).

Together, these give a complete charge balance on the system, specifying not only the composition, but also the doping level and the intrinsic/extrinsic ion pairing. With this information, the  $T_g$  is then compared against the water/intrinsic ion pair ratio. Interestingly, it is shown that the same correlation holds true for three separate systems: PDADMA-PSS PECs, PDADMA-PSS PEMs, and PAH-PAA PECs. This spans weak and strong polyelectrolytes, as well as multilayers and complexes, which indicates the general role of water in controlling the glass transition in polyelectrolyte assemblies.

## RESULTS AND DISCUSSION

To fully correlate the  $T_g$  with the physical structure of the PEC, it is necessary to do a charge balance on the system, from which the doping level can be deduced. The doping level is an expression of the extrinsic ion pairing, whereby the process of doping with salt ions destroys intrinsic ion pairs and creates extrinsic ion pairs. Figure 2 shows the compositions of PECs prepared and isolated from stoichiometric (1:1 by repeat unit) mixtures of PDADMA and PSS in the presence of various salt concentrations (see also Supporting Information, Figure S3). From NAA, the PDADMA and PSS compositions were calculated, Figure 2a. For PECs at all salt concentrations, PDADMA was in excess at 52–55 mol %, which is attributed to differences in linear charge density and hydrophilicity of PDADMA and PSS.<sup>15</sup> It is likely that uncomplexed polyelectrolyte was removed during the centrifugation step. This nonstoichiometric composition has also been observed elsewhere using scintillation counting.<sup>37</sup>

The salt doping process of PECs is represented in the Supporting Information, eq S1. Due to the observed nonstoichiometry of the PECs, the salt doping level  $y$ , indicating the fraction of extrinsic sites, in Supporting Information, eq S2, was divided into cationic and anionic doping level contributions:

$$y^+ = \frac{[\text{Cl}^-]}{[\text{PDADMA}]}; y^- = \frac{[\text{Na}^+]}{[\text{PSS}]} \quad (1)$$

NAA allowed for the estimation of these doping levels  $y^+$  and  $y^-$  (Figure 2b) by measuring the elemental  $\text{Na}^+$  and  $\text{Cl}^-$  concentration in the PEC. If all  $\text{Na}^+$  and  $\text{Cl}^-$  ions are assumed to participate in extrinsic ion pairing, then  $y$  may be considered equivalent to the fraction of extrinsic polyelectrolyte repeat units. The doping level,  $y^+$  and  $y^-$ , generally increased with increasing complexation salt concentration up to 1 M. A complexation concentration of 1.5 M NaCl resulted in a

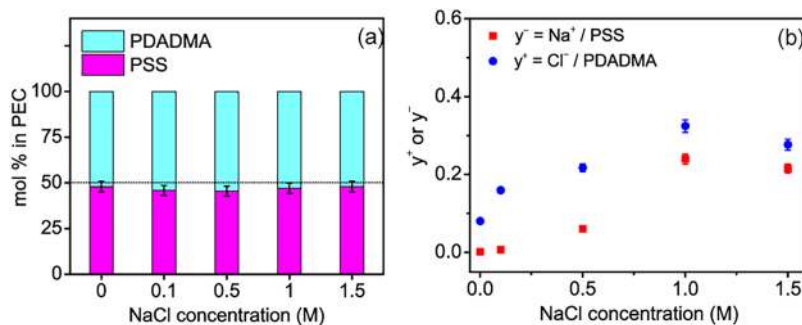


**Figure 2.** (a) PEC composition based on PDADMA and PSS repeat units for PECs prepared at varying NaCl concentrations measured. (b) Doping levels, for which  $y^-$  and  $y^+$  are the molar ratios of  $\text{Na}^+$  to PSS and  $\text{Cl}^-$  to PDADMA, respectively. The error bars represent the uncertainties (95% confidence level).

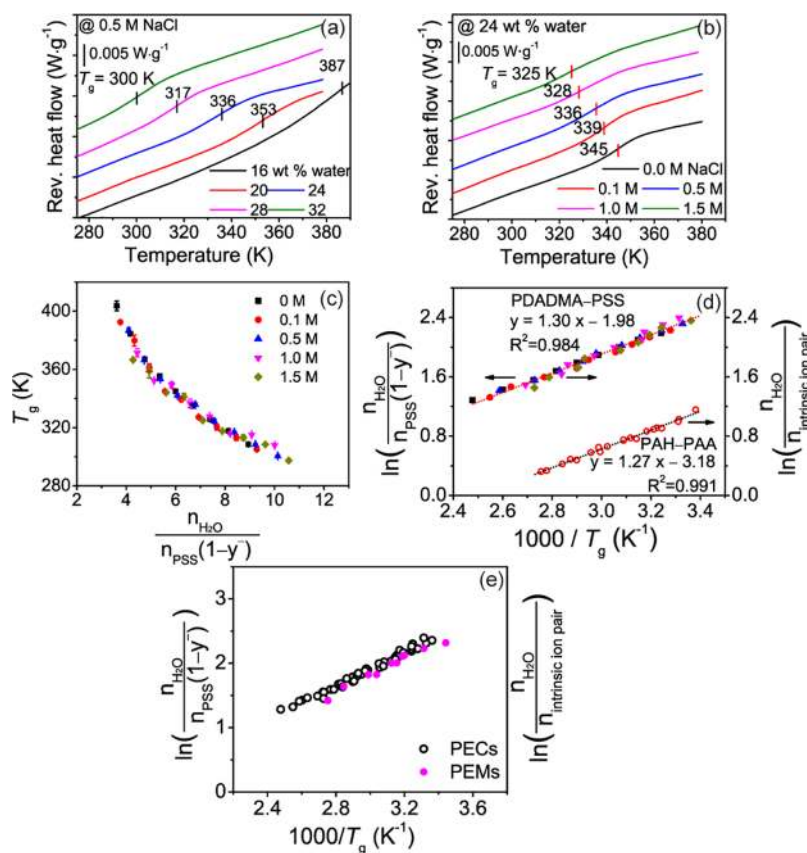


**Figure 3.** Reversing heat flow curves for PDADMA–PSS PECs of (a) varying water content and fixed 0.5 M NaCl complexation concentration, and (b) varying NaCl complexation concentration and fixed water content of 24 wt %. (c)  $T_g$  as a function of the molar ratio of water molecules to intrinsic ion pair in hydrated PDADMA–PSS complexes prepared from solutions of different NaCl concentrations. (d) Linear fitting of  $\ln(n_{\text{H}_2\text{O}}/n_{\text{intrinsic ion pair}})$  vs  $1000/T_g$  (dotted lines). For (a) and (b), second heating scans are shown with “exotherm down”, heating at  $2 \text{ K}\cdot\text{min}^{-1}$ , amplitude of  $1.272 \text{ K}$  for a period of 60 s. The legend in (c) also applies to (d). The left y-axis applies to PDADMA–PSS, and the right y-axis applies to both PDADMA–PSS and PAH–PAA. PAH–PAA data are from the authors’ previous work.<sup>35</sup> (e)  $\ln(n_{\text{H}_2\text{O}}/n_{\text{intrinsic ion pair}})$  vs  $1000/T_g$  for PDADMA–PSS polyelectrolyte complexes (PECs, black circles) and polyelectrolyte multilayers (PEMs, pink circles).

decreased doping level, but the meaning of this particular result is circumspect on account of the extreme softness of the material and the tendency of the PEC to lose salt during the isolation procedure. In all PECs,  $y^+$  was greater than  $y^-$ , which can be explained by the excess PDADMA in the PECs. The trend observed here using NAA most closely mimics that observed using inductively coupled plasma mass spectrometry (ICP-MS) and conductivity, Figure S4.<sup>21,38</sup>

The effect of hydration on the PEC’s  $T_g$  was examined using modulated DSC, Figure 3a. The inflection point of the sigmoidal reversing heat flow response was assigned as  $T_g$ . For a fixed complexation salt concentration of 0.5 M,  $T_g$  decreased from 387 to 300 K as water content increased from 16 to 32 wt %. An enthalpic relaxation peak in the nonreversing heat flow curve was also present, Figure S5a. For comparison, a dried PEC exhibited no remarkable thermal features, Figure S5b.

Water contributes to PEC plasticization via (1) enhancing free volume which facilitates polymer chain motion,<sup>33,39–42</sup> (2) lubricating the polymer chains by decreasing the internal resistance of polymer sliding motions,<sup>33,43</sup> and (3) decreasing electrostatic attractions between polyelectrolyte intrinsic ion pairs. Whereas the first two effects are associated with traditional plasticization,<sup>39,42</sup> the last effect in polyelectrolyte complexes and assemblies makes water a nontraditional

plasticizer, analogous to salt. Zhang et al. observed that the direct contact number of intrinsic ion pairs decreased as water content increased.<sup>41</sup> Elsewhere, organic alcohol solvents (*n*-butanol, ethylene glycol, 1-propanol, and propanediol) bore no plasticization effect on PECs or PEMs.<sup>35,36</sup>

Figure 3b shows the response for PECs of varying complexation NaCl concentration at a fixed hydration level of 24 wt %.  $T_g$  decreased from 345 to 325 K as the NaCl concentration increased from 0 to 1.5 M, indicative of a salt-plasticization effect. Doping has an intense local effect on screening between intrinsic ion pairs, which decreases physical cross-linking and increases polymer mobility.<sup>44–47</sup> This is consistent with the trend in doping levels displayed in Figure 2b.

The effects of hydration and salt on the  $T_g$  are summarized in Figure S6. As shown, the effect of salt doping on the  $T_g$  is much less pronounced than the effect of hydration. This emphasizes the general trend that  $T_g$  decreases with increasing water content and complexation NaCl concentration, confirming the plasticizing effect of water,<sup>32,33,35</sup> and also the effects of salt doping, which breaks intrinsic ion pairs and lowers the  $T_g$ .<sup>21,41</sup> For example, salt-time superpositioning of PECs has demonstrated strong effects on dynamic behavior.<sup>48</sup> The question is, then, how water and doping are together quantifiably interrelated to the glass transition.

Recently, the molar ratio of water molecules to intrinsic ion pairs has been suggested to control  $T_g$  (or  $T_{tr}$ )<sup>35</sup> in PAH–PAA complexes. Also, water and salt influence PAH–PAA complexation behavior.<sup>49</sup> To explore water–salt–temperature relations for the PDADMA–PSS system,  $T_g$  values for PDADMA–PSS complexes were plotted against the ratio of water molecules to intrinsic ion pairs  $\frac{n_{H_2O}}{n_{intrinsic\ ion\ pair}}$ , Figure 3c. The water content  $n_{H_2O}$  was taken as the controlled amount of water added to the system, and  $n_{intrinsic\ ion\ pair}$  was taken from the charge balance and the doping level. This  $\frac{n_{H_2O}}{n_{intrinsic\ ion\ pair}}$  ratio can also be expressed in terms of the doping level  $y^+$  or  $y^-$ , depending on which species is a minority. Here, the molar ratio of water to intrinsic ion pairs becomes  $\frac{n_{H_2O}}{n_{PSS}(1-y^-)}$ . Remarkably, the  $T_g$  values all collapsed into a single master curve for all hydration levels and salt concentrations examined.

Figure 3d shows the linearization of this master curve in the form of  $\ln\left(\frac{n_{H_2O}}{n_{intrinsic\ ion\ pair}}\right) = 1.30 \times (1000/T_g) - 1.98$  ( $R^2 = 0.984$ ).

This relationship provides an energy of  $-10.8\text{ kJ}\cdot\text{mol}^{-1}$ , which is close in value to the van't Hoff enthalpy  $\Delta H$  associated with the disruption of one O–H $\cdots$ O unit ( $10.5 \pm 2.5\text{ kJ}\cdot\text{mol}^{-1}$ ).<sup>50</sup> This possibly suggests a link between the glass transition and hydrogen bond distribution in PECs. The enthalpy is also similar to values obtained from the proton conductivity of polymer membranes and Nafion nanofibers.<sup>51,52</sup> The successful collapse and linearization of  $T_g$  values for PDADMA–PSS complexes is notably similar to that observed in PAH–PAA complexes, shown in Figure 3d for comparison, with an energy of  $-10.5\text{ kJ}\cdot\text{mol}^{-1}$ .<sup>35</sup> The slopes and energies for both types of complexes are similar, which further suggests the generalized role of water in the relaxation. It is curious that the  $y$ -intercepts for the linear fits in Figure 3d are different for PDADMA–PSS and PAH–PAA PECs. The difference may be attributed to the differences in charged group size or ion pair size (e.g., PDADMA repeat unit is larger than PAH repeat unit), linear charge density, and/or the water distribution around the charged groups between these two PEC systems. The significance of the  $y$ -intercept is a focus of ongoing work.

These results show generalized behavior between two very different types of PECs (strong vs weak), yet there still remains the question of if this behavior is similar for charged assemblies made by a different path. To examine this, we performed the same analysis for PDADMA–PSS PEMs made using the layer-by-layer assembly technique. Whereas PECs are made here by the rapid mixing of polycation and polyanion solutions, PEMs are made by the alternate and sequential adsorption of polycations and polyanions from solution to a surface. PEMs can possess stratified or mixed structures,<sup>53,54</sup> and the assembly conditions here were selected so as to give a more mixed structure within the layers. PDADMA–PSS PEMs were exposed to various salt concentrations and water contents, and their  $T_g$ 's were measured. Elemental analysis was performed as before to obtain the doping level and intrinsic/extrinsic ion pair content. The results, plotted in Figure 3e, show the nearly perfect overlay of PEM and PEC behavior. The first heating scans from PECs and PEMs also show the same results (Figure S7). Despite being formed by very different methods, the manner in which water controls the  $T_g$  appears to be essentially the same, pointing to similar local environments.

Therefore, this master curve identifies a unifying parameter, namely, the molar ratio of water to intrinsic ion pairs, that

controls the  $T_g$  in charged assemblies and reflects the roles of both water and ionization. The  $T_g$  for PECs and PEMs is concluded to follow the general relationship:

$$1/T_g \sim \ln\left(\frac{n_{H_2O}}{n_{intrinsic\ ion\ pair}}\right) \quad (2)$$

Molecular dynamics (MD) calculations in all-atom detail were performed to further investigate the water distribution and molecular interactions that give rise to the behavior at the  $T_g$ . Figure 4 displays a simulated PEC structure and the

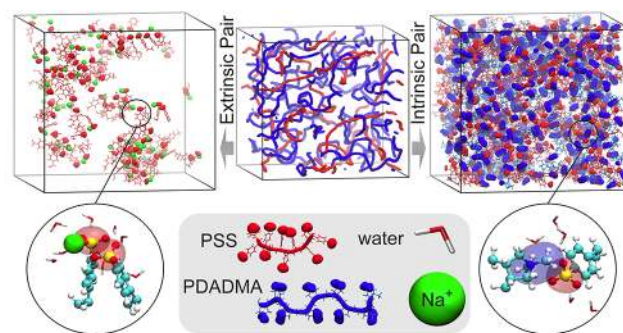


**Figure 4.** Representative snapshot of a hydrated PDADMA–PSS complex, prepared from 1.5 M NaCl solution first and then hydrated with 30 wt % water and its extrinsic (left) and intrinsic (right) ion pairs.

visualizations of extrinsic and intrinsic ion pairs corresponding to 1.5 M NaCl concentration and 30 wt % water. The magnification of an extrinsic pair site shows a  $\text{Na}^+$  counterion surrounded by multiple charged PSS groups, demonstrating a three-dimensional packing configuration. Due to this three-dimensional packing character, a specific polyelectrolyte site can bear both intrinsic and extrinsic charge compensation character, see Supporting Information. Figure S8 compares the mole fraction of intrinsically compensated PSS groups calculated from simulations and experiments; the generally good agreement between the experimental and simulation approaches supports the validity of the quantitative calculation in Figure 3.

The distribution and location of water molecules in the PECs were further investigated. The analysis focused on the PSS group because our recent work on PDADMA/PSS assemblies has shown indications that the observed thermal transition behavior is linked with shortening of the hydrogen bond lifetime between PSS and water.<sup>36</sup> Upon heating, water experiences faster rotation and vibration movements, as indicated by the shortening of H-bond lifetime and increase of molecular diffusion coefficient.<sup>36,41</sup> The data in Figure 5a,b show that the total number of water–sulfonate hydrogen bonds decreases with increasing temperature and that the decrease results dominantly from water at the intrinsic ion pairs. For extrinsically compensated ion pairs, the number of hydrogen bonds with water was relatively insensitive to temperature, Figure 5c. Likely, this results from the  $\text{Na}^+$  ion in the extrinsic ion pairs pinning nearby water molecules. The number of intrinsically charge compensated ion pairs exceeded the number of extrinsically compensated ones, see Figure 4, so the decrease in the total water–sulfonate hydrogen bonds tracks closely with that of the intrinsic ion pairs. The PSS hydration shell size (in water molecules) depended on hydration, salt concentration,

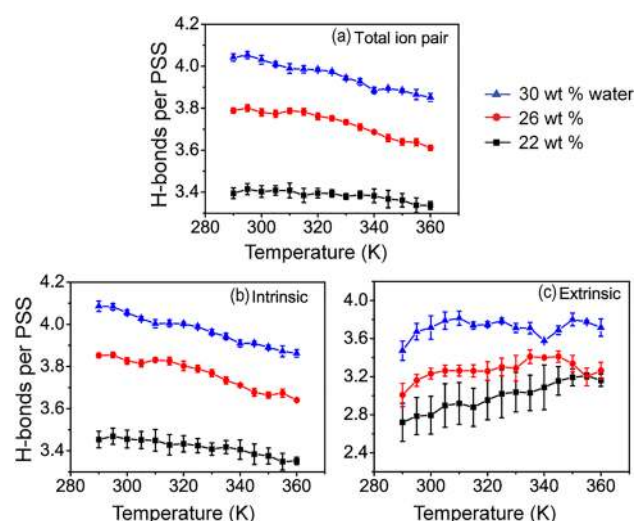


**Figure 5.** PSS–water hydrogen bond analysis for simulations of PECs of different water content prepared from 0.5 M NaCl solution (a) total, (b) intrinsically, and (c) extrinsically compensated ion pairing of PSS. Panels (a–c) correspond to the average of three simulations.

and whether the PSS sulfonate group was intrinsically or extrinsically compensated, Figure S9.

In prior simulation work, a clear transition in the lifetime, and consequently the number of hydrogen bonds between PSS sulfonate groups and water, was observed and interpreted to be associated with the thermal transition or  $T_g$ .<sup>36</sup> The data shown in Figure 5a,b correspond to a much larger simulation system, so the transition here was relatively weak. Individual simulation runs are presented in Figure S10. The plot in Figure 5c presents the insensitivity of hydrogen bonds between water and extrinsically compensated PSS. These molecular simulations show the partitioning of water to intrinsic and extrinsic sites, specifically the water-activated  $T_g$  at the intrinsic ion pair.

## CONCLUSION

The origin of how water at the intrinsic ion pair facilitates the relaxation of charged polyelectrolyte assemblies has been demonstrated. The fact that the scaling of  $1/T_g \sim \ln\left(\frac{n_{\text{H}_2\text{O}}}{n_{\text{intrinsic ion pair}}}\right)$  experimentally applied to pH-sensitive and salt-sensitive systems, as well as systems made by different approaches, points to water's generalized role. This scaling gave identical energies of  $\sim -10.8$  kJ/mol, similar in value to the van't Hoff enthalpy of a hydrogen bond,<sup>50</sup> for all charged polyelectrolyte assemblies. MD simulations of PDADMA–PSS directly observed the intrinsic and extrinsic ion pairs separately, showing that the  $T_g$  was connected to a decrease in H-bonds between water–PSS at intrinsic ion pairs. These findings imply an underlying mechanism for the glass transition: water plasticizes the PECs by weakening intrinsic ion pairing and water surrounding the intrinsic ion pair facilitates the sliding motion and relaxation of polyelectrolytes within the assembly. These findings may potentially be generalized to any aqueous macromolecular assembly containing charged ion pairs, whether that be natural or synthetic.

## ASSOCIATED CONTENT

### Supporting Information

The Supporting Information is available free of charge on the ACS Publications website at DOI: 10.1021/acscentsci.8b00137.

Experimental and simulation procedures, neutron activation analysis (NAA), <sup>1</sup>H NMR spectroscopy, comparison of current and previous work on salt doping level, DSC thermograms and results of hydrated and dried PECs, first heating scans of PECs and PEMs, calculated and experimental values of ion pairing, number of water molecules in the first hydration shell of PSS, individual simulation runs of PECs (PDF)

## AUTHOR INFORMATION

### Corresponding Authors

\* (J.L.L.) E-mail: jodie.lutkenhaus@tamu.edu.

\* (M.S.) E-mail: maria.sammalkorpi@aalto.fi.

### ORCID

Yanpu Zhang: 0000-0002-8555-6539

Piotr Batys: 0000-0002-2264-3053

Fei Li: 0000-0002-4177-2539

Maria Sammalkorpi: 0000-0002-9248-430X

Jodie L. Lutkenhaus: 0000-0002-2613-6016

### Notes

The authors declare no competing financial interest.

## ACKNOWLEDGMENTS

The authors acknowledge the financial support of the National Science Foundation under Grant No. 1609696 (J.L.L.) and Academy of Finland Grant No. 309324 (M.S.). The authors acknowledge CSC – IT Center for Science, Finland, for computational resources. We also thank Dr. Bryan Tomlin of Center for Chemical Characterization and Analysis, Texas A&M University, for advice with NAA data analysis.

## REFERENCES

- (1) Müller-Späh, S.; Soranno, A.; Hirschfeld, V.; Hofmann, H.; Rügger, S.; Reymond, L.; Nettels, D.; Schuler, B. Charge interactions can dominate the dimensions of intrinsically disordered proteins. *Proc. Natl. Acad. Sci. U. S. A.* **2010**, *107* (33), 14609.
- (2) Pinheiro, A. V.; Han, D.; Shih, W. M.; Yan, H. Challenges and opportunities for structural DNA nanotechnology. *Nat. Nanotechnol.* **2011**, *6* (12), 763.
- (3) Zhang, D. Y.; Seelig, G. Dynamic DNA nanotechnology using strand-displacement reactions. *Nat. Chem.* **2011**, *3*, 103.
- (4) Zhao, X.; Pan, F.; Xu, H.; Yaseen, M.; Shan, H.; Hauser, C. A. E.; Zhang, S.; Lu, J. R. Molecular self-assembly and applications of designer peptide amphiphiles. *Chem. Soc. Rev.* **2010**, *39* (9), 3480.
- (5) Richardson, J. J.; Björnalm, M.; Caruso, F. Technology-driven layer-by-layer assembly of nanofilms. *Science* **2015**, *348* (6233), aaa2491.
- (6) Boudou, T.; Crouzier, T.; Ren, K.; Blin, G.; Picart, C. Multiple Functionalities of Polyelectrolyte Multilayer Films: New Biomedical Applications. *Adv. Mater.* **2010**, *22* (4), 441.
- (7) Michaels, A. S. Polyelectrolyte Complexes. *Ind. Eng. Chem.* **1965**, *57* (10), 32.
- (8) van der Gucht, J.; Spruijt, E.; Lemmers, M.; Cohen Stuart, M. A. Polyelectrolyte complexes: Bulk phases and colloidal systems. *J. Colloid Interface Sci.* **2011**, *361* (2), 407.
- (9) Liu, X.; Haddou, M.; Grillo, I.; Mana, Z.; Chapel, J. P.; Schatz, C. Early stage kinetics of polyelectrolyte complex coacervation monitored through stopped-flow light scattering. *Soft Matter* **2016**, *12* (44), 9030.
- (10) Cohen Stuart, M. A.; Besseling, N. A. M.; Fokink, R. G. Formation of micelles with complex coacervate cores. *Langmuir* **1998**, *14* (24), 6846.
- (11) Dautzenberg, H. Polyelectrolyte complex formation in highly aggregating systems. 1. Effect of salt: polyelectrolyte complex

formation in the presence of NaCl. *Macromolecules* **1997**, *30* (25), 7810.

(12) Perry, S. L.; Sing, C. E. PRISM-Based Theory of Complex Coacervation: Excluded Volume versus Chain Correlation. *Macromolecules* **2015**, *48* (14), 5040.

(13) Qin, J.; de Pablo, J. J. Criticality and Connectivity in Macromolecular Charge Complexation. *Macromolecules* **2016**, *49* (22), 8789.

(14) Perry, S. L.; Li, Y.; Priftis, D.; Leon, L.; Tirrell, M. The effect of salt on the complex coacervation of vinyl polyelectrolytes. *Polymers* **2014**, *6* (6), 1756.

(15) Zhang, Y.; Yildirim, E.; Antila, H. S.; Valenzuela, L. D.; Sammalkorpi, M.; Lutkenhaus, J. L. The influence of ionic strength and mixing ratio on the colloidal stability of PDAC/PSS polyelectrolyte complexes. *Soft Matter* **2015**, *11* (37), 7392.

(16) Zhang, H.; Wang, C.; Zhu, G.; Zacharia, N. S. Self-Healing of Bulk Polyelectrolyte Complex Material as a Function of pH and Salt. *ACS Appl. Mater. Interfaces* **2016**, *8* (39), 26258.

(17) Shah, N. J.; Hyder, M. N.; Quadir, M. A.; Dorval Courchesne, N.-M.; Seeherman, H. J.; Nevins, M.; Spector, M.; Hammond, P. T. Adaptive growth factor delivery from a polyelectrolyte coating promotes synergistic bone tissue repair and reconstruction. *Proc. Natl. Acad. Sci. U. S. A.* **2014**, *111* (35), 12847.

(18) Kremer, T.; Kováčević, D.; Salopek, J.; Požar, J. Conditions Leading to Polyelectrolyte Complex Overcharging in Solution: Complexation of Poly (acrylate) Anion with Poly (allylammonium) Cation. *Macromolecules* **2016**, *49* (22), 8672.

(19) Laaser, J. E.; Lohmann, E.; Jiang, Y.; Reineke, T. M.; Lodge, T. P. Architecture-Dependent Stabilization of Polyelectrolyte Complexes between Polyanions and Cationic Triblock Terpolymer Micelles. *Macromolecules* **2016**, *49* (17), 6644.

(20) Imre, Á. W.; Schönhoff, M.; Cramer, C. Unconventional Scaling of Electrical Conductivity Spectra for PSS-PDADMAC Polyelectrolyte Complexes. *Phys. Rev. Lett.* **2009**, *102* (25), 255901.

(21) Shamoun, R. F.; Hariri, H. H.; Ghostine, R. A.; Schlenoff, J. B. Thermal Transformations in Extruded Saloplastic Polyelectrolyte Complexes. *Macromolecules* **2012**, *45* (24), 9759.

(22) Cohen Stuart, M. A.; Huck, W. T. S.; Genzer, J.; Muller, M.; Ober, C.; Stamm, M.; Sukhorukov, G. B.; Szleifer, I.; Tsukruk, V. V.; Urban, M.; et al. Emerging applications of stimuli-responsive polymer materials. *Nat. Mater.* **2010**, *9* (2), 101.

(23) Jaber, J. A.; Schlenoff, J. B. Polyelectrolyte Multilayers with Reversible Thermal Responsivity. *Macromolecules* **2005**, *38* (4), 1300.

(24) Köhler, K.; Möhwald, H.; Sukhorukov, G. B. Thermal Behavior of Polyelectrolyte Multilayer Microcapsules: 2. Insight into Molecular Mechanisms for the PDADMAC/PSS System. *J. Phys. Chem. B* **2006**, *110* (47), 24002.

(25) Köhler, K.; Shchukin, D. G.; Möhwald, H.; Sukhorukov, G. B. Thermal Behavior of Polyelectrolyte Multilayer Microcapsules. 1. The Effect of Odd and Even Layer Number. *J. Phys. Chem. B* **2005**, *109* (39), 18250.

(26) Vidyasagar, A.; Sung, C.; Gamble, R.; Lutkenhaus, J. L. Thermal Transitions in Dry and Hydrated Layer-by-Layer Assemblies Exhibiting Linear and Exponential Growth. *ACS Nano* **2012**, *6* (7), 6174.

(27) Sung, C.; Hearn, K.; Lutkenhaus, J. Thermal transitions in hydrated layer-by-layer assemblies observed using electrochemical impedance spectroscopy. *Soft Matter* **2014**, *10* (34), 6467.

(28) Krebs, T.; Tan, H. L.; Andersson, G.; Morgner, H.; Van Patten, P. G. Increased layer interdiffusion in polyelectrolyte films upon annealing in water and aqueous salt solutions. *Phys. Chem. Chem. Phys.* **2006**, *8* (46), 5462.

(29) Nolte, A. J.; Treat, N. D.; Cohen, R. E.; Rubner, M. F. Effect of Relative Humidity on the Young's Modulus of Polyelectrolyte Multilayer Films and Related Nonionic Polymers. *Macromolecules* **2008**, *41* (15), 5793.

(30) Gu, Y.; Zacharia, N. S. Self-Healing Actuating Adhesive Based on Polyelectrolyte Multilayers. *Adv. Funct. Mater.* **2015**, *25* (24), 3785.

(31) Gu, Y.; Weinheimer, E. K.; Ji, X.; Wiener, C. G.; Zacharia, N. S. Response of Swelling Behavior of Weak Branched Poly(ethylene imine)/Poly(acrylic acid) Polyelectrolyte Multilayers to Thermal Treatment. *Langmuir* **2016**, *32* (24), 6020.

(32) Lyu, X.; Clark, B.; Peterson, A. M. Thermal transitions in and structures of dried polyelectrolytes and polyelectrolyte complexes. *J. Polym. Sci., Part B: Polym. Phys.* **2017**, *55* (8), 684.

(33) Hariri, H. H.; Lehaf, A. M.; Schlenoff, J. B. Mechanical properties of osmotically stressed polyelectrolyte complexes and multilayers: Water as a plasticizer. *Macromolecules* **2012**, *45* (23), 9364.

(34) Fu, J.; Abbett, R. L.; Fares, H. M.; Schlenoff, J. B. Water and the Glass Transition Temperature in a Polyelectrolyte Complex. *ACS Macro Lett.* **2017**, *6* (10), 1114.

(35) Zhang, Y.; Li, F.; Valenzuela, L. D.; Sammalkorpi, M.; Lutkenhaus, J. L. Effect of Water on the Thermal Transition Observed in Poly (allylamine hydrochloride)–Poly (acrylic acid) Complexes. *Macromolecules* **2016**, *49* (19), 7563.

(36) Yildirim, E.; Zhang, Y.; Lutkenhaus, J. L.; Sammalkorpi, M. Thermal Transitions in Polyelectrolyte Assemblies Occur via a Dehydration Mechanism. *ACS Macro Lett.* **2015**, *4* (9), 1017.

(37) Fu, J.; Fares, H. M.; Schlenoff, J. B. Ion-Pairing Strength in Polyelectrolyte Complexes. *Macromolecules* **2017**, *50* (3), 1066.

(38) Zhang, B.; Hoagland, D. A.; Su, Z. Ionic Liquids as Plasticizers for Polyelectrolyte Complexes. *J. Phys. Chem. B* **2015**, *119* (8), 3603.

(39) Wypych, G. *Handbook of Plasticizers*; ChemTec Publishing: Toronto, 2004.

(40) Immergut, E. H.; Mark, H. F. Principles of Plasticization. In *Plasticization and Plasticizer Processes*; American Chemical Society: Washington, DC, 1965; Vol. 48.

(41) Zhang, R.; Zhang, Y.; Antila, H. S.; Lutkenhaus, J. L.; Sammalkorpi, M. Role of Salt and Water in the Plasticization of PDAC/PSS Polyelectrolyte Assemblies. *J. Phys. Chem. B* **2017**, *121* (1), 322.

(42) Hodge, R. M.; Bastow, T. J.; Edward, G. H.; Simon, G. P.; Hill, A. J. Free Volume and the Mechanism of Plasticization in Water-Swollen Poly(vinyl alcohol). *Macromolecules* **1996**, *29* (25), 8137.

(43) McCormick, M.; Smith, R. N.; Graf, R.; Barrett, C. J.; Reven, L.; Spiess, H. W. NMR Studies of the Effect of Adsorbed Water on Polyelectrolyte Multilayer Films in the Solid State. *Macromolecules* **2003**, *36* (10), 3616.

(44) Jaber, J. A.; Schlenoff, J. B. Mechanical Properties of Reversibly Cross-Linked Ultrathin Polyelectrolyte Complexes. *J. Am. Chem. Soc.* **2006**, *128* (9), 2940.

(45) Volodkin, D.; von Klitzing, R. Competing mechanisms in polyelectrolyte multilayer formation and swelling: Polycation–polyanion pairing vs. polyelectrolyte–ion pairing. *Curr. Opin. Colloid Interface Sci.* **2014**, *19* (1), 25.

(46) Fu, J.; Schlenoff, J. B. Driving Forces for Oppositely Charged Polyion Association in Aqueous Solutions: Enthalpic, Entropic, but Not Electrostatic. *J. Am. Chem. Soc.* **2016**, *138* (3), 980.

(47) Selin, V.; Ankner, J. F.; Sukhishvili, S. A. Diffusional Response of Layer-by-Layer Assembled Polyelectrolyte Chains to Salt Annealing. *Macromolecules* **2015**, *48* (12), 3983.

(48) Spruijt, E.; Sprakel, J.; Lemmers, M.; Stuart, M. A. C.; van der Gucht, J. Relaxation Dynamics at Different Time Scales in Electrostatic Complexes: Time-Salt Superposition. *Phys. Rev. Lett.* **2010**, *105* (20), 208301.

(49) Chollakup, R.; Smithipong, W.; Eisenbach, C. D.; Tirrell, M. Phase Behavior and Coacervation of Aqueous Poly(acrylic acid)–Poly(allylamine) Solutions. *Macromolecules* **2010**, *43* (5), 2518.

(50) Walrafen, G. E. Raman Spectral Studies of H<sub>2</sub>O in H<sub>2</sub>O. *J. Chem. Phys.* **1968**, *48* (1), 244.

(51) Chen, L.; Hallinan, D. T.; Elabd, Y. A.; Hillmyer, M. A. Highly Selective Polymer Electrolyte Membranes from Reactive Block Polymers. *Macromolecules* **2009**, *42* (16), 6075.

(52) Dong, B.; Gwee, L.; Salas-de la Cruz, D.; Winey, K. I.; Elabd, Y. A. Super Proton Conductive High-Purity Nafion Nanofibers. *Nano Lett.* **2010**, *10* (9), 3785.

(53) McAloney, R. A.; Sinyor, M.; Dudnik, V.; Goh, M. C. Atomic Force Microscopy Studies of Salt Effects on Polyelectrolyte Multilayer Film Morphology. *Langmuir* **2001**, *17* (21), 6655.

(54) Klitzing, R. v. Internal structure of polyelectrolyte multilayer assemblies. *Phys. Chem. Chem. Phys.* **2006**, *8* (43), 5012.